Taylor & Francis
Taylor & Francis Group

Biofouling
The Journal of Bioadhesion and Biofilm Research

ISSN: 0892-7014 (Print) 1029-2454 (Online) Journal homepage: www.tandfonline.com/journals/gbif20

Attachment point theory revisited: the fouling response to a microtextured matrix

A. J. Scardino, J. Guenther & R. de Nys

To cite this article: A. J. Scardino, J. Guenther & R. de Nys (2008) Attachment point theory revisited: the fouling response to a microtextured matrix, Biofouling, 24:1, 45-53, DOI: 10.1080/08927010701784391

To link to this article: https://doi.org/10.1080/08927010701784391

Biofouling
Vol. 24, No. 1, January 2008, 45–53

Taylor & Francis
Taylor & Francis Group

Attachment point theory revisited: the fouling response to a microtextured matrix

A.J. Scardino[a,b]*, J. Guenther[b] and R. de Nys[b]

[a]*Maritime Platforms Division, Defence Science & Technology Organisation, Melbourne, Victoria, Australia;* [b]*School of Marine & Tropical Biology, James Cook University, Townsville, Queensland, Australia*

(*Received 1 August 2007; accepted 30 October 2007*)

This paper examines attachment point theory in detail by testing the fouling attachment of several fouling groups to a microtextured matrix. Static bioassays were conducted on polycarbonate plates with nine equal regions, comprising eight scales of microtexture (4–512 μm) and one untextured region. The microtextures examined were continuous sinusoidal ridges and troughs of defined height and width. Attachment over the microtextured plates was examined for the diatom *Amphora* sp., the green alga *Ulva rigida*, the red alga *Centroceras clavulatum*, the serpulid tube worm *Hydroides elegans* and the bryozoan *Bugula neritina*. It was found that the size of the microtexture in relation to the size of the settling propagules/larvae was important in the selection of attachment sites. Attachment was generally lower when the microtexture wavelength was slightly smaller than the width of the settling propagules/larvae and increased when the wavelength was wider than their width. The effect of attachment points was weak for small motile microfoulers (*Amphora* sp. and *U. rigida*) (7 μm), strong for large macrofouling larvae (*H. elegans* and *B. neritina*) (129–321 μm) and non-existent for the non-motile algal spores (*C. clavulatum*) (37 μm). This study reinforces the potential of using attachment points to develop surfaces with increased fouling resistance or, alternatively, surfaces which promote the attachment of selected target sizes of motile propagules or larvae.

Keywords: attachment points; microtexture; non-toxic antifouling; selected attachment; invertebrate larvae; algal propagules; diatoms

Introduction

The study of surface microtexture has gained momentum in recent years with the discovery of naturally fouling resistant organisms that display surface microtexture (Wahl et al. 1998; Ball 1999; Baum et al. 2002; Scardino et al. 2003; Bers and Wahl 2004). Artificial surfaces have been produced that are inspired from natural microtextures, and these biomimics have provided promising fouling resistance (Figueiredo et al. 1997; Bers and Wahl 2004; Scardino and de Nys 2004; Bers et al. 2006). In addition, designed microfabricated surfaces have been tested against diatoms (Scardino et al. 2006), algal spores (Callow et al. 2002; Hoipkemeier-Wilson et al. 2005; Carman et al. 2006; Schumacher et al. 2007b) and barnacle cyprid larvae (Berntsson et al. 2000b; Petronis et al. 2000). These organisms demonstrate mixed attachment (in this case referring to attachment of diatoms, settlement and germination of algae, and settlement and metamorphosis of larvae) preferences depending on the size of the organism tested and the microtexture of the surface. While the variation in attachment on surface structures is well documented, the mechanism of action of how microtexture affects fouling is not well understood. Attachment point theory has been proposed as a possible mechanism for reduced or increased fouling on microtextured surfaces, whereby fouling organism attachment is increased when there are optimal numbers of 'potential settling points' (Hills et al. 1999) or 'attachment points' (Callow et al. 2002) and reduced with few (sub-optimal) points of attachment (Scardino et al. 2006). The number of attachment points is dependent on the size of the settling larvae/spores and the wavelength of the microtexture. Attachment to microtextures/microrefuges has been explored for barnacle cyprids (Lemire and Bourget 1996; Hills et al. 1999; Köhler et al. 1999; Lapointe and Bourget 1999; Berntsson et al. 2000a; Petronis et al. 2000) and *Ulva* spores (Callow et al. 2002; Hoipkemeier-Wilson et al. 2004). These studies have found that for cyprids of various barnacle species, attachment is reduced on microgrooves and pyramids below the size of the cyprid. Similarly, *Ulva* spore attachment is increased on microtextures slightly larger than the spore size. Attachment preferences also affect adhesion strength. Microrefuges have been shown to be important in protecting *Ulva linza* spores from hydrodynamic forces, reducing spore removal. These refuges occur when the spore is slightly smaller than the size of the microtexture (Granhag et al. 2004; Hoipkemeier-Wilson et al. 2004).

*Corresponding author. Email: Andrew.Scardino@dsto.defence.gov.au

ISSN 0892-7014 print/ISSN 1029-2454 online

DOI: 10.1080/08927010701784391
http://www.informaworld.com

Refuge is also sought in areas of small scale heterogeneity by *Bugula neritina* larvae (Walters 1992; Walters and Wethey 1996).

The concept of attachment point theory is illustrated in Scardino et al. (2006). For several diatom species, attachment was reduced on surfaces with texture below the size of the cell, while attachment increased on smooth surfaces and when textures provided multiple numbers of attachment points. The present study expands on these findings (Scardino et al. 2006) and tests major fouling classes comprising a wide range of cell, larvae and propagule sizes (7–321 μm) for attachment preferences across a broad range of microtexture wavelengths (4–512 μm). The aim of this study was to determine if attachment point theory holds for broad classes of fouling larvae and algal propagules in static choice bioassays. The five fouling organisms used are the raphid diatom *Amphora* sp., the green alga *Ulva rigida*, the red alga *Centroceras clavulatum*, the serpulid *Hydroides elegans* and the bryozoan *Bugula neritina*. *Amphora* sp. contacts the surface passively, attaches via the excretion of extracellular polymeric substances and can glide across a surface. *U. rigida* gametes have flagella and can move freely across a surface to explore. Attachment is initiated by the secretion of a glycoprotein adhesive, which rapidly cures on the surface. After this process, the gamete is non-motile (Finlay et al. 2002). Red algal spores (*C. clavulatum*) have no flagella and hence contact the surface passively, after which mucilage and adhesive vesicles are released. *H. elegans* larvae are motile and require a stimulus to metamorphose (biofilm or chemical) (Bryan et al. 1997; Carpizo-Ituarte and Hadfield 1998; Pechenik and Qian 1998). Upon reaching a suitable surface, larvae secrete a primary tube, resorb the prototroch cilia, form a collar which secretes the secondary, calcified tube, and the adult feeding tentacles emerge. This process can take <12 h (Hadfield 1998). *B. neritina* larvae are freely motile (for several hours) due to an external covering of cilia. Larvae adhere to the surface through adhesive secretions from the pyriform groove and internal sac, which becomes extruded and forms a permanent disc-like holdfast (Mawatari 1951).

Methods

Ablation of polymers

A matrix of microtextured patterns was manufactured by MiniFAB Pty Ltd in 1.5 mm polycarbonate by laser micromachining using an excimer laser system (8000 series, Exitech, UK) equipped with a Lambda Physik LPX210i laser source operating at a wavelength of 248 nm with krypton fluoride (KrF) as the excitation gas. The master template for the polycarbonate pieces was 100 × 100 mm and consisted of nine 30 × 30 mm squares, each with a sinusoidal shaped pattern, which varied in both the period (distance from peak to peak) and depth (distance from peak to trough) of the sinusoidal shape (Figure 1).

Full details of the machining process used to produce the microtextured matrix are detailed in Harvey and Rumsby (1997). In brief, it involved delivering a laser beam onto a chrome-on-quartz mask. The mask was controlled by an X-Y stage allowing precise lateral and vertical movement. The microtextured polycarbonate master copy was metallised after laser machining. An inverse copy of this master was subsequently electroformed in nickel using a nickel sulphamate bath (Harvey and Rumsby 1997). This nickel tool was then used as a master for replicating several microtextured parts in polycarbonate by hot embossing. Each polycarbonate piece was arranged as displayed in Figure 1 and listed in Table 1. The eight different texture widths were 4, 8, 16, 32, 64, 128, 256 and 512 μm. The centre square was unmachined polycarbonate.

Surface characterisation

All microtextures were assessed for accuracy using scanning electron microscopy. For aspect ratios,

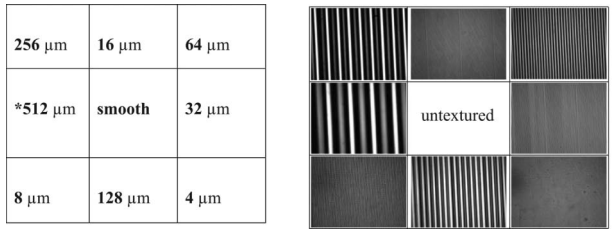

Figure 1. The arrangement of microtextured squares on the polycarbonate matrix. The number in each square represents the depth and period of microtexture with the exception of the *512 μm microtextured square, which has a period of 512 μm and a depth of 256 μm due to machining constraints.

Table 1. Summary of the surface characterisation of microtextured polycarbonate.

Wavelength (μm)	Depth (μm)	Aspect ratio	Wettability (°)
Smooth	0	1:1	70.9 ± 3.4
4	4–6	1:1	69.3 ± 3.3
8	4–6	1:1	71.3 ± 4.2
16	14	1:1	84.3 ± 1.2
32	30	1:1	100.5 ± 7.5
64	59	1:1	84.0 ± 4.6
128	125	1:1	69.4 ± 4.3
256	245	1:1	82.1 ± 6.9
512	256	1:0.5	78.3 ± 2

microtextured depths were determined using an optical microscope (50× objective). Wettabilities of each texture and control (unmodified PC) of polycarbonate were determined using the sessile drop method, by measuring advancing water contact angles using a goniometer (Rahme-Hart, NRL-CA, 100-00). Three replicate drops (2 µl) were used for each surface texture. The aspect ratio between the microtextured wavelength and depth was kept constant at 1:1 except for the 512-µm texture, which could not be manufactured at a 1:1 ratio and had a 1:0.5 ratio (width:depth). The wettability of microtextured squares varied between all textures and the smooth polycarbonate (69°–100°) (Table 1).

Collection of organisms

Five fouling species were used in bioassays on microtextured polycarbonate plates. They were the benthic raphid diatom *Amphora* sp. (CS-255), the green alga *Ulva rigida* (C. Agardh), the red alga *Centroceras clavulatum* (C. Agardh) Montagne, the serpulid tube worm *Hydroides elegans* (Haswell) and the bryozoan *Bugula neritina* Linneaus.

Amphora sp. (CS-255) (Class Bacillariophyceae, Order Bacillariales) stock cultures were obtained from CSIRO microalgal supply service, Tasmania, Australia, and assays were conducted at James Cook University (JCU) laboratories.

The algae *C. clavulatum* and *U. rigida* were collected from intertidal rock pools at North Clovelly, Sydney (33° 55′S; 151° 15′E). A variety of plants from different areas on the rock platforms were collected and placed in bags with *in situ* seawater and returned immediately to the laboratory at the University of New South Wales (UNSW) for assays. For *Ulva*, the presence of reproductive thalli was checked each day for 2 weeks before a full moon.

For the serpulid *H. elegans*, adult specimens were collected from settlement plates at the Breakwater Marina, Townsville (19° 16′S, 146° 49′E).

The bryozoan *B. neritina* is a cosmopolitan species occurring along the eastern Australian coastline. Bioassays were conducted at UNSW. Colonies of *B. neritina* were collected from boat hulls at Rose Bay, Sydney (33° 53′S; 151° 15′E) and placed in bags with *in situ* seawater and returned immediately to the laboratory.

Bioassay procedures

Amphora *sp. (CS-255)*

Growth conditions for *Amphora* sp. (width 7 µm, length 14 µm) were 12:12 light:dark cycle with a light intensity of 80 µmol photons PAR m^{-2} s^{-1}, using Philips daylight or cool white fluorescent tubes. Diatom cultures were supplemented with F2 medium (Guillard and Ryland 1962). *Amphora* sp. was cultured at 25°C. The cells were re-suspended with an orbital shaker and their concentration determined using a haemocytometer prior to use in assays. The test surfaces were rinsed in filtered (0.2 µm) seawater before adding diatom cultures. Plastic weigh-boats, 120 × 120 mm, were used to contain the microtextured polycarbonate settlement plates in all assays. The dishes were filled with 120 ml of filtered (0.2 µm) seawater, and 150 µl of diatom culture suspension were pipetted into each textured square with a cell density of approximately 1.6×10^5 cells ml^{-1}. Five replicate microtextured pieces were used. The diatoms were left to attach for 3 h, after which they were dip-rinsed and counted in 10 random fields of view (FOV) per dish at magnifications of 400× (0.16 mm^2). The dip-rinsing involved immersing each treatment in a new beaker of filtered (0.2 µm) seawater three times to remove unattached cells. The surfaces were briefly exposed to air during this process (the technique used in Scardino et al. 2006).

U. rigida

Fertile thalli (with yellow tips) of *U. rigida* were kept in seawater under refrigeration for 2 h after collection. They were then dried and placed in new seawater and exposed to light. Gametes (two terminally inserted flagella) (diameter 7 µm) were released after 15 min and swam towards the light. A suspension of gametes was pipetted into a separate beaker under light and stirred to prevent settlement until the solution was light green in colour. Approximately 150 µl (6.3×10^5 cells) were added to each dish with a microtextured polycarbonate plate with 120 ml of filtered (0.2 µm) seawater. Gametes were left to settle and germinate for 96 h, after which the dishes were dip-rinsed and the number of plants counted in 5 FOV (×200, 0.64 mm^2) on each microtextured square. There were five replicate microtextured polycarbonate plates.

C. clavulatum

Collected plants were brought to the laboratory and checked under a dissecting microscope for cystocarps, which were removed and placed in a separate dish. Spores were released from the cystocarps (diameter 37 µm) over 30–60 min. Approximately 100 spores were randomly pipetted into each dish with a microtextured polycarbonate plate with 120 ml of filtered (0.2 µm) seawater. The spores were left to germinate over 48 h, after which the dishes were dip-rinsed and the numbers of

plants were counted on each microtextured square. Six replicate microtextured polycarbonate plates were used.

H. elegans

Adult specimens were placed in Petri dishes containing filtered (0.45 μm) seawater. Their tubes were gently broken, after which gametes were released. Fertilized eggs were allowed to develop for 30 min and were then transferred to 2-l aerated glass beakers containing 0.45 μm FSW. Larvae were cultured at 10 larvae ml^{-1} and fed *Isochrysis* sp. (CS-177, CSIRO) at 6×10^4 algal cells ml^{-1} for 5 days, after which larvae were competent to settle. As *H. elegans* larvae do not settle unless a settlement cue is provided, isobutyl methylxanthine (IBMX, Sigma-Aldrich) was used to induce settlement (Bryan et al. 1997; Lau and Qian 1997). To promote larval settlement, 120 ml of 10^{-4} M IBMX in filtered (0.45 μm) seawater and 200 larvae (width 129 μm, length 235 μm) were added to each dish. The dishes were kept under temperature and light control for 48 h. Subsequently, settled and metamorphosed larvae having calcified tubes and tentacles were counted with a dissecting microscope. There were five replicate dishes.

B. neritina

Colonies of *B. neritina* were placed in aerated seawater in the dark for 24 h after collection. After approximately 15 min exposure to light, larvae (diameter 321 μm) were released and pipetted into each dish with a microtextured polycarbonate plate with 120 ml of filtered (0.2 μm) seawater. Approximately 100 larvae were placed in each dish, covered and allowed to settle in the dark for 24 h. After this time, the number of settled and metamorphosed larvae in each microtextured square was recorded. There were five replicate dishes.

For all bioassays, three un-machined control pieces of polycarbonate were used to ensure cells, propagules and larvae were competent to attach to this material and that there was an even spread of attachment across the polycarbonate piece (no clumping in certain areas).

Measurement of cells, propagules and larvae

All diatoms, gametes, spores and larvae were photographed (Leica, DC300 camera) and sizes were measured with the measurement module of the image analysis program IM50 (Leica Microsystems). Ten replicates were measured for each species.

Statistical analysis

Analysis of attachment between microtextures was done using analysis of variance (ANOVA, $\alpha = 0.05$), followed by Tukey's HSD multiple comparison tests (SPSS version 12). Dish was included as a blocked factor as textures in one dish were not independent. There was no interaction term (texture × dish) in the analyses because textures were not replicated in each dish. The assumptions of homogeneity and normality of the data were checked with scattergrams of standardized residuals versus predicted means and Q-Q plots of standardized residuals, respectively (Underwood 1981). Where assumptions were not met, data were transformed (arcsine square-root).

Results

Cell, propagule and larval sizes

Larvae, propagule and cell sizes from the organisms chosen provide a broad range of sizes for the testing of microtextured polycarbonate (Table 1). The smallest organisms were the *Amphora* sp. cells (width 7.0 μm) and *U. rigida* gametes (7.24 μm diameter), *C. clavulatum* spores were 37.5 μm, *H. elegans* larvae were 129.4 μm whilst *B. neritina* larvae were much larger (321.5 μm) (sizes listed in Table 2) (hereafter all sizes are to the nearest μm).

Amphora *sp. assay*

The *Amphora* sp. cells were 7 μm wide and 14 μm long and could fit inside all textures except the 4 μm. The mean proportion of *Amphora* sp. cells attached to the microtextured squares was not significantly different ($F_{8,32} = 0.918$, $p = 0.527$, Figure 2). The texture with the lowest proportion of *Amphora* sp. cells was 512 μm with 7.9% (46.4 ± 19.2 cells per FOV) and 4 μm with

Table 2. Cell, propagule and larval sizes of fouling organisms used in bioassays.

Larval/cell size	*Amphora* sp.	*U. rigida*	*C. clavulatum*	*H. elegans*	*B. neritina*
Width (μm)	7.3 ± 0.26	7.2 ± 0.13	37.5 ± 1.8	129.0 ± 3.2	321.4 ± 5.1
Length (μm)	14.0 ± 0.1	N/A spherical	N/A spherical	234.8 ± 4.4	N/A spherical

Data are means ± SE.

9.18% (49.3 ± 19.4 cells per FOV) of cells attached to these textures. In contrast, the 8-μm texture, which is slightly larger than the width of *Amphora* sp. cells, had the highest proportion of attached cells, 14.7% (88.3 ± 43 cells per FOV) (Figure 2).

U. rigida *assay*

U. rigida gametes had a mean width of 7 μm and could fit inside all textures except the 4 μm. The proportion of *U. rigida* gametes settled and germinated on the untextured and microtextured squares was not significantly different ($F_{8,32} = 4.657$, $p = 0.544$, Figure 3). The texture with the highest proportion of settled and germinated *U. rigida* gametes was 64 μm, which had 16.7% (76.2 ± 34.5 gametes per FOV) of gametes attached to this texture. In contrast, the 4-μm texture, the only texture smaller than the *U. rigida* spore size, had the lowest proportion of settled and germinated gametes, 5.4% (16.12 ± 4.34 gametes per FOV) (Figure 3). The number of gametes settled and germinated increased with increasing texture widths up to 64 μm, then decreased for the largest three microtextures. Gametes settled and germinated in moderate numbers on the untextured polycarbonate (20.8 ± 3.4 gametes per FOV).

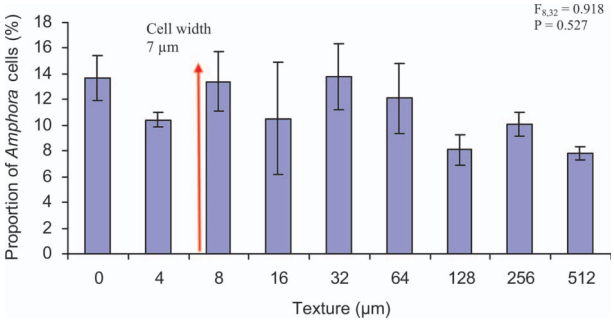

Figure 2. The proportion of *Amphora* sp. cells attached to microtextured squares. Data are means ± SE ($n = 5$), and analysis was done by ANOVA. The vertical bar indicates the mean width of *Amphora* sp. cells.

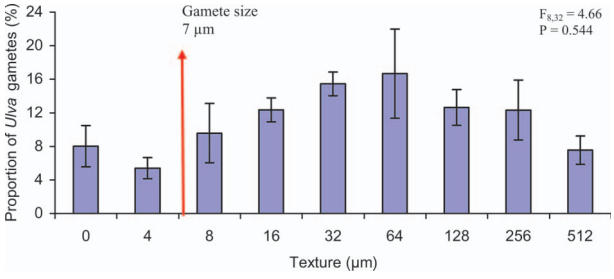

Figure 3. The proportion of settled and germinated *U. rigida* gametes on microtextured squares. Data are means ± SE ($n = 5$), and analysis was done by ANOVA. The vertical bar indicates the mean width of *U. rigida* gametes.

C. clavulatum *assay*

The spore size was 37 μm (diameter) and therefore could fit inside all textures above 32 μm. However, *C. clavulatum* spores are non-motile. The number of *C. clavulatum* spores settled and germinated on the microtextured squares was not significantly different ($F_{8,32} = 2.971$, $p = 0.589$, Figure 4). The highest *C. clavulatum* germination occurred on the untextured polycarbonate (21.8 ± 12.3 spores), whilst the lowest germination occurred on the 256 μm microtexture (6.3 ± 3.2 spores). The proportion of spores settled and germinated was similar across all textures, ranging from 9.1% to 10.9% (Figure 4).

H. elegans *assay*

H. elegans larvae have a mean width of 129 μm and can therefore fit inside the 256 μm and 512 μm textures. The proportion of *H. elegans* larvae settled and metamorphosed on the microtextured squares was significantly different ($F_{8,32} = 4.66$, $p = 0.001$, Figure 5). The highest proportion of settled and metamorphosed *H. elegans* larvae was on the largest ripples 512 μm (26.7% ± 3.7%, 12 larvae) and 256 μm (24.8% ± 1.9%, 10 larvae), which are the only textures larger than the larvae. In contrast, significantly fewer larvae settled and metamorphosed on all the microtextures below the width of the larvae, with the exception of the 16 μm texture, which was not significantly different to the 256-μm texture. The lowest settlement occurred on the 4-μm (0.8% ± 0.6%), 32-μm (1.2% ± 0.5%) and 64-μm textures (1.4% ± 0.2%). Settlement on all textures below the width of the larvae was not significantly different from each other.

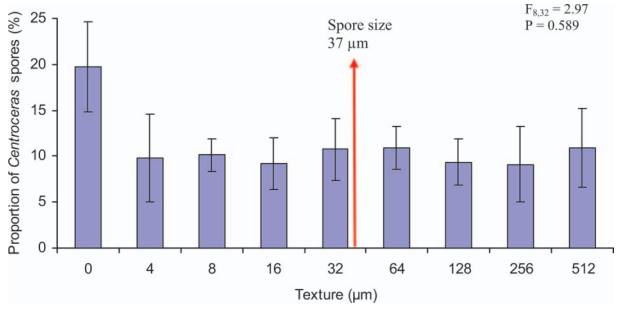

Figure 4. The proportion of settled and germinated *C. clavulatum* spores on microtextured squares. Data are means ± SE ($n = 6$), and analysis was done by ANOVA. The vertical bar indicates the mean diameter of *C. clavulatum* spores.

B. neritina *assay*

The size of *B. neritina* larvae was 321 μm and therefore could only fit inside the 512-μm texture. The proportion of *B. neritina* larvae settled and metamorphosed on the microtextured squares was significantly different ($F_{8,32} = 2.21$, $p = 0.036$, Figure 6). The highest proportion of settled and metamorphosed *B. neritina* larvae was on the largest ripples 512 μm (23.4% ± 6.7%, 36 larvae), which is the only texture larger than the larvae. In contrast, significantly fewer larvae settled and metamorphosed to the 64-μm and 256-μm textures (5.3% ± 2.7%, 16 larvae and 5.8% ± 2.8%, 17 larvae, respectively). Settlement and metamorphosis on all the remaining textures ranged from 8.5% to 15% and was not significantly different to settlement and metamorphosis on any other textures.

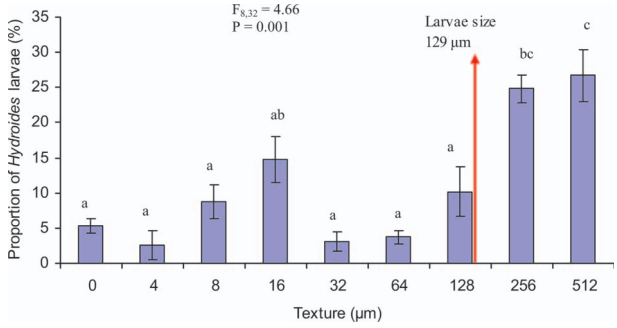

Figure 5. The proportion of settled and metamorphosed *H. elegans* larvae on microtextured squares. Data are means ± SE ($n = 5$), and analysis was done by ANOVA followed by Tukey's *post hoc* test. Columns with a dissimilar letter are significantly different at $\alpha = 0.05$. The vertical bar indicates the mean width of *H. elegans* larvae.

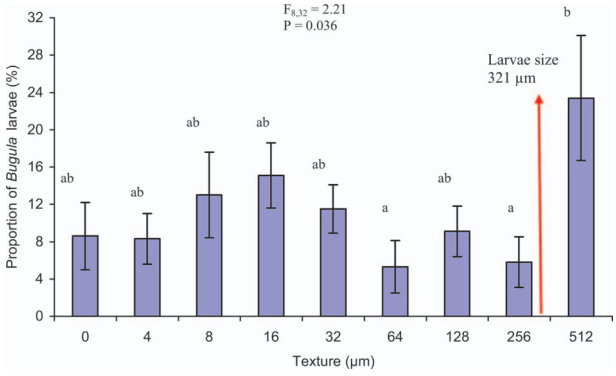

Figure 6. Proportions of settled and metamorphosed *B. neritina* larvae to microtextured squares. Data are means ± SE ($n = 5$), and analysis was done by one-way ANOVA followed by Tukey's *post hoc* test. Columns with a dissimilar letter are significantly different at $\alpha = 0.05$. The vertical bar indicates the mean width of *B. neritina* larvae.

Discussion

The fouling organisms chosen in this study cover the major groups of fouling classes and larval/propagule sizes and demonstrate the influence of attachment points and surface microtexture on attachment. There is a broad range of attachment preferences by the different fouling organisms to varying scales of microtexture (in this case referring to attachment of diatoms, settlement and germination of algae, and settlement and metamorphosis of larvae). Overall, there was a general trend for fouling species to attach in lower numbers to microtextures slightly smaller than the width of the organism, and in greater numbers on microtextures wider than the organism. However, significant effects of microtexture on attachment were detected for only two of the five species examined. The effects of attachment points on settlement were weak on motile microfoulers (*Amphora* and *Ulva*), strong on macrofouling larvae (*Hydroides* and *Bugula*) and non-existent for non-motile algal spores (*Centroceras*). For *Amphora* sp. (cell size 7 μm), attachment was lower on the 4-μm texture and higher on the 8-μm texture and *U. rigida* (gamete size 7 μm) attached in lower numbers on the 4-μm texture. However, these differences were not significant. *H. elegans* (larval size 129 μm) attached in significantly lower numbers on the 128-μm texture, and in significantly higher numbers on the 256-μm and 512-μm texture. *B. neritina* (larval size 321 μm) attachment was significantly lower on the 256-μm texture and significantly higher on the 512-μm texture. These findings provide species-specific support for attachment point theory (Table 3).

Surface microtexture has previously been tested against *Amphora* sp. (Scardino et al. 2006), *U. linza* (Callow et al. 2002; Hoipkemeier-Wilson et al. 2004) and *Balanus* species (Hills et al. 1999; Berntsson et al. 2000a, b; Petronis et al. 2000). *Amphora* sp.

Table 3. Summary of attachment to microtextured polycarbonate for each species tested.

Species	Size (μm)	Attachment to first texture smaller than cell size	Attachment to first texture larger than cell size
Amphora sp.	7	(4 μm) Lower	(8 μm) Higher
U. rigida	7	(4 μm) Lower	(8 μm) Equal
C. clavulatum	37	(32 μm) Equal	(64 μm) Equal
H. elegans	129	(128 μm) Lower*	(256 μm) Higher*
B. neritina	321	(256 μm) Lower*	(512 μm) Higher*

Lower, lower proportion of cells attached compared to other microtextures; Higher, a greater proportion of cells attached compared to other microtextures; Equal, a similar proportion of cells attached compared to other microtextures; *a significant difference in attached cells between microtextures at $\alpha = 0.05$.

attachment numbers were reduced compared to smooth controls on microtextured surfaces smaller than the width of the cell (Scardino et al. 2006). Whilst this finding is consistent with the present study in which the 7 μm *Amphora* sp. cells attached in fewer numbers on the 4-μm texture, compared to larger microtextures and a smooth control, the differences in this study were not significant. This is possibly due to the greater range of choices (eight textures and a smooth control) compared to the previous no choice bioassays.

U. linza spores have been reported to prefer microtextures slightly larger than the spore size (Callow et al. 2002; Hoipkemeier-Wilson et al. 2004), while in this study *U. rigida* showed no such preference. However, attachment was lower (non-significant) on microtexture slightly smaller (4 μm) than the spore size. Both *Amphora* cells and *Ulva* gametes attached in relatively higher numbers to textures larger than their size. This pattern of settlement could be due to the sinusoidal shape of the microtexture, which allows for attachment at the bottom of the texture, even though the top of the channel becomes wider. Square channels with an even width throughout the depth of the channel may be better to determine the effect of size of texture on attachment. It has been shown recently that the aspect ratio is an important factor in the attachment of *U. linza* (Schumacher et al. 2007a). In this study, aspect ratio was kept constant at a ratio of 1:1.

Several studies have shown that *Balanus improvisus* cyprids are deterred by microtextures smaller than the cyprid size (250–270 μm) (Berntsson et al. 2000a; Petronis et al. 2000), while Hills et al. (1999) found that densities of *Semibalanus balanoides* were positively correlated to Potential Settling Sites (PSS). Although barnacle cyprids were not tested in this study, similar trends were found for bryozoan larvae, which are of a similar size. *B. neritina* larvae fitted to attachment point theory, as there was significantly lower attachment on the 256-μm texture compared to the 512-μm texture. *B. neritina* larvae are known to prefer small-scale heterogeneity where refuge is often found (Walters 1992; Walters and Wethey 1996). Whilst the smallest scale of surface complexity chosen in those studies was in the order of millimeters, it supports the present finding that *B. neritina* larvae prefer textures larger than their body size.

Consistent with the result for *B. neritina*, *H. elegans* larvae settled in higher numbers on the textures larger than their width (256 and 512 μm). The serpulid *H. elegans* is a cosmopolitan fouling organism settling on most man-made structures. Whilst it is well known that serpulid larvae settle in response to biofilmed surfaces (Carpizo-Ituarte and Hadfield 1998; Beckmann et al. 1999; Unabia and Hadfield 1999), little is known about the settlement preferences in relation to surface texture and attachment points. Walters et al. (1997) found that *H. elegans* larvae are not gregarious in laboratory assays and do not actively seek crevices. However, in the field more larvae settled in crevices than expected by chance. It is thought that due to hydrodynamics larvae are transported passively to small scale eddies created by already established tubeworms and settle in the crevices between the tube wall and the substratum (Walters et al. 1997). In this study, *H. elegans* larvae favour textures larger than their width and have lower settlement on the sizes slightly less than their width when given a choice of a range of microtextures.

Supporting the concept of selective settlement based on the ability to attach, spores of the red alga *C. clavulatum* settle passively, drifting onto a surface rather than actively exploring it. It would be expected that all areas of the textured plate have an even number of attached spores. Any differences in settlement would reflect changes in adhesion strength resulting from the dip-rinsing process. Considering that the spores do not choose where to settle, it was particularly interesting to see if the attachment point theory would fit for this species. Spores of *C. clavulatum* did not conform to attachment point theory as expected, as spore attachment was similar on all microtextures, with the highest attachment occurring on untextured polycarbonate.

Each fouling organism was tested on untextured polycarbonate controls to ensure competency to attach to this material. As each polycarbonate piece was designed with the same texture pattern arrangement, cells, larvae and propagules were also checked to ensure there was no settlement to conspecifics, or clumping, on certain areas of the polycarbonate piece, thereby ensuring that any observed differences were due to changes in texture and not edge effects. However, the etching of the microtextures onto polycarbonate altered the wettability of the surface (70°–100°) and this may affect the settlement density of algal spores. *Ulva* spores are known to settle in increasing densities as surface energy is reduced (Callow et al. 2000), and this preference for more hydrophobic surfaces could explain the increased settlement densities on the 32-, 64- and 256-μm textures, which also have the highest contact angles.

This study has given support to attachment point theory, in that organisms will attach in lower numbers when there are fewer potential attachment points. The next important research direction will be to determine the attachment strength on microtextures above and below the scale of the fouling organisms. Given the potential dampening effect of the curved surface on attachment points, it would also be useful to test the

sizes in this study using alternative shapes, such as square-edged grooves, to remove bias for attachment at the base of larger sinusoidal surfaces. Previous work on adhesion strength under flow has demonstrated the importance of microtopographies/surface roughness on larval and spore removal (Berntsson et al. 2000b; Schultz et al. 2000; Schultz and Swain 2000; Finlay et al. 2002; Granhag et al. 2004). Depending on the scale of roughness or topography relative to the fouling organism, protection from hydrodynamic forces can occur. For spores of *U. linza* (size 5 μm), lower removal after exposure to a water jet was found on microtopographies with profile heights of 25 and 36 μm compared to smooth and large scale topographies (Granhag et al. 2004), while microtextures 5 μm wide and 5 μm deep (a perfect fit for spores) had the lowest spore removal after exposure to a flow channel (Hoipkemeier-Wilson et al. 2004). In contrast, microtopographies at a similar scale (30–45 μm) reduced barnacle attachment (Berntsson et al. 2000 a, b) and in this case topography was smaller than the scale of the fouling organism and did not provide a refuge from hydrodynamics.

The forces required to remove fouling larvae from surface microtexture are an important consideration for the development of fouling-release technologies. Finlay et al. (2002) demonstrated that on a smooth surface (glass) the surface pressure required to remove *U. linza* spores after 4 h is 250 kPa, and this increases substantially with time. It is therefore unlikely that spores would be removed under operating speeds of most vessels. With many antifouling surfaces moving towards foul-release, rather than non-stick coatings, it is important that surface roughness/microtexture does not increase adhesion strength and the forces required for fouling removal. A surface with fewer attachment points, and one which does not provide microrefuges, may reduce the shear forces required for fouling removal, and therefore would be an excellent foul-release candidate. Finally, *in situ*, fouling larvae and propagules come in all sizes, and as such a successful surface will need a combination of microtextures with fractal dimensions to cover microfouling and macrofouling organisms (Schumacher et al. 2007a). The applicability of attachment point theory and the influence of surface microtexture against multispecies fouling consortia in laboratory trials incorporating flow, and in field trials, is now the next step in assessing the longer-term efficiency of microfabricated biomimics.

Acknowledgements

The authors would like to thank Rick Barber and the MiniFAB staff for the production of the microtextured surfaces. Peter Steinberg kindly provided support for work at UNSW. Louise McKenzie, Nick Paul and Paul Gribben provided support to experiments conducted at UNSW. Financial assistance was provided by the Biomimetic Fouling Control Program, Maritime Platforms Division, Defence Science Technology Organisation, Australia.

References

Ball P. 1999. Engineering – shark skin and other solutions. Nature. 400:507–509.

Baum C, Meyer W, Stelzer R, Fleischer L-G, Siebers D. 2002. Average nanorough skin surface of the pilot whale (*Globicephala melas*, Delphinidae): considerations on the self-cleaning abilities based on nanoroughness. Mar Biol. 140:653–657.

Beckmann M, Harder T, Qian PY. 1999. Induction of larval attachment and metamorphosis in the serpulid polychaete *Hydroides elegans* by dissolved free amino acids: mode of action in laboratory bioassays. Mar Ecol Prog Ser. 190:167–178.

Berntsson KM, Jonsson PR, Lejhall M, Gatenholm P. 2000a. Analysis of behavioural rejection of microtextured surfaces and implications for recruitment by the barnacle *Balanus improvisus*. J Exp Mar Biol Ecol. 251:59–83.

Berntsson KM, Andreasson H, Jonsson PR, Larsson L, Ring K, Petronis S, Gatenholm P. 2000b. Reduction of barnacle recruitment on micro-textured surfaces: analysis of effective topographic characteristics and evaluation of skin friction. Biofouling. 16:245–261.

Bers AV, Wahl M. 2004. The influence of natural surface microtopographies on fouling. Biofouling. 20:43–51.

Bers AV, Prendergast GS, Zurn CM, Hansson L, Head RM, Thomason JC. 2006. A comparative study of the anti-settlement properties of mytilid shells. Biol Lett. 2:88–91.

Bryan PJ, Qian PY, Kreider JL, Chia FS. 1997. Induction of larval settlement and metamorphosis by pharmacological and conspecific associated compounds in the serpulid polychaete *Hydroides elegans*. Mar Ecol Prog Ser. 146:81–90.

Callow ME, Callow JA, Ista LK, Coleman SE, Nolasco AC, Lopez GP. 2000. Use of self-assembled monolayers of different wettabilities to study surface selection and primary adhesion processes of green algal (*Enteromorpha*) zoospores. Appl Environ Microbiol. 66:3249–3254.

Callow ME, Jennings AR, Brennan AB, Seegert CE, Gibson A, Wilson L, Feinberg A, Baney R, Callow JA. 2002. Microtopographic cues for settlement of zoospores of the green fouling alga *Enteromorpha*. Biofouling. 18:237–245.

Carman ML, Estes TG, Feinberg AW, Schumacher JF, Wilkerson W, Wilson LH, Callow ME, Callow JA, Brennan AB. 2006. Engineered antifouling microtopographies – correlating wettability with cell attachment. Biofouling. 22:11–21.

Carpizo-Ituarte E, Hadfield MG. 1998. Stimulation of metamorphosis in the polychaete *Hydroides elegans* Haswell (Serpulidae). Biol Bull. 194:14–24.

Figueiredo M, Norton TA, Kain JM. 1997. Settlement and survival of epiphytes on two intertidal crustose coralline alga. J Exp Mar Biol Ecol. 213:247–260.

Finlay JA, Callow ME, Schultz MP, Swain GW, Callow JA. 2002. Adhesion strength of settled spores of the green alga *Enteromorpha*. Biofouling. 18:251–256.

Granhag LM, Finlay JA, Jonsson PR, Callow JA, Callow ME. 2004. Roughness-dependent removal of settled spores of the green alga *Ulva* (syn. *Enteromorpha*) exposed to hydrodynamic forces from a water jet. Biofouling. 20:117–122.

Guillard RRL, Ryland JH. 1962. Studies on marine planktonic diatoms. I. *Cyclotella nana* Hustedt and *Detonula confervacea* (Cleve). Can J Microbiol. 8:229–239.

Hadfield MG. 1998. The DP Wilson Lecture. Research on settlement and metamorphosis of marine invertebrate larvae: past, present and future. Biofouling. 12:9–29.

Harvey EC, Rumsby PT. 1997. Fabrication techniques and their applications to produce novel micromachined structures using excimer laser projection. Proc SPIE: Int Soc Optical Eng. 3223:26–33.

Hills JM, Thomason JC, Muhl J. 1999. Settlement of barnacle larvae is governed by euclidean and not fractal surface characteristics. Funct Ecol. 13:868–875.

Hoipkemeier-Wilson L, Schumacher JF, Finlay JA, Perry R, Callow ME, Callow JA, Brennan AB. 2005. Towards minimally fouling substrates: surface grafting and topography. Polym Preprint. 46:1312–1313.

Hoipkemeier-Wilson L, Schumacher JF, Carman ML, Gibson AL, Feinberg AW, Callow ME, Finlay JA, Callow JA, Brennan AB. 2004. Antifouling potential of lubricious, micro-engineered, PDMS elastomers against zoospores of the green alga *Ulva* (*Enteromorpha*). Biofouling. 20:53–63.

Köhler J, Hansen PD, Wahl M. 1999. Colonization patterns at the substratum-water interface: how does surface microtopography influence recruitment patterns of sessile organisms? Biofouling. 14:237–248.

Lapointe L, Bourget E. 1999. Influence of substratum heterogeneity scales and complexity on a temperate epibenthic marine community. Mar Ecol Prog Ser. 189:159–170.

Lau SCK, Qian PY. 1997. Phlorotannins and related compounds as larval settlement inhibitors of the tube-building polychaete *Hydroides elegans*. Mar Ecol Prog Ser. 159:219–227.

Lemire M, Bourget E. 1996. Substratum heterogeneity and complexity influence micro-habitat selection of *Balanus* sp. and *Tubularia crocea* larvae. Mar Ecol Prog Ser. 135:77–87.

Mawatari S. 1951. The natural history of the common fouling bryozoan *Bugula neritina* (Linneaus). Miscellaneous Report from the Research Institute for Natural Resources Tokyo. p. 47–54. Nos 19–21.

Pechenik JA, Qian PY. 1998. Onset and maintenance of metamorphic competence in the marine polychaete *Hydroides elegans* Haswell in response to three chemical cues. J Exp Mar Biol Ecol. 226:51–74.

Petronis S, Berntsson K, Gold J, Gatenholm P. 2000. Design and microstructuring of PDMS surfaces for improved marine biofouling resistance. J Biomater Sci: Polym Ed. 11:1051–1072.

Scardino AJ, de Nys R. 2004. Fouling deterrence on the bivalve shell *Mytilus galloprovincialis*: a physical phenomenon? Biofouling. 20:249–257.

Scardino AJ, Harvey E, de Nys R. 2006. Testing attachment point theory: diatom attachment on microtextured polyimide biomimics. Biofouling. 22:55–60.

Scardino A, de Nys R, Ison O, O'Connor W, Steinberg P. 2003. Microtopography and antifouling properties of the shell surface of the bivalve molluscs *Mytilis galloprovincialis* and *Pinctada imbricata*. Biofouling. 19:221–230.

Schultz MP, Swain GW. 2000. The influence of biofilms on skin friction drag. Biofouling. 15:129–139.

Schultz MP, Finlay JA, Callow ME, Callow JA. 2000. A turbulent channel flow apparatus for the determination of the adhesion strength of microfouling organisms. Biofouling. 15:243–251.

Schumacher JF, Aldred N, Callow ME, Finlay JA, Callow JA, Clare AS, Brennan AB. 2007a. Species-specific engineered antifouling topographies: correlations between the settlement of algal zoospores and barnacle cyprids. Biofouling. 23:307–317.

Schumacher JF, Carman ML, Estes TG, Feinberg AW, Wilson LH, Callow ME, Callow JA, Finlay JA, Brennan AB. 2007b. Engineered antifouling microtopographies – effect of feature size, geometry, and roughness on settlement of zoospores of the green alga *Ulva*. Biofouling. 23:55–62.

Unabia CRC, Hadfield MG. 1999. Role of bacteria in larval settlement and metamorphosis of the polychaete *Hydroides elegans*. Mar Biol. 133:55–64.

Underwood AJ. 1981. Techniques of analysis of variance in experimental marine biology and ecology. Oceanogr Mar Biol. 19:513–605.

Wahl M, Kroeger K, Lenz M. 1998. Non-toxic protection against epibiosis. Biofouling. 12:1–3.

Walters LJ. 1992. Postsettlement success of the arborescent bryozoan *Bugula neritina* (L) – the importance of structural complexity. J Exp Mar Biol Ecol. 164:55–71.

Walters LJ, Wethey DS. 1996. Settlement and early post-settlement survival of sessile marine invertebrates on topographically complex surfaces: the importance of refuge dimensions and adult morphology. Mar Ecol Prog Ser. 137:1–3.

Walters LJ, Hadfield MG, delCarmen KA. 1997. The importance of larval choice and hydrodynamics in creating aggregations of *Hydroides elegans* (Polychaeta: Serpulidae). Invert Bio1. 16:102–114.